Supporting Information

Buckley et al. 10.1073/pnas.0910827107

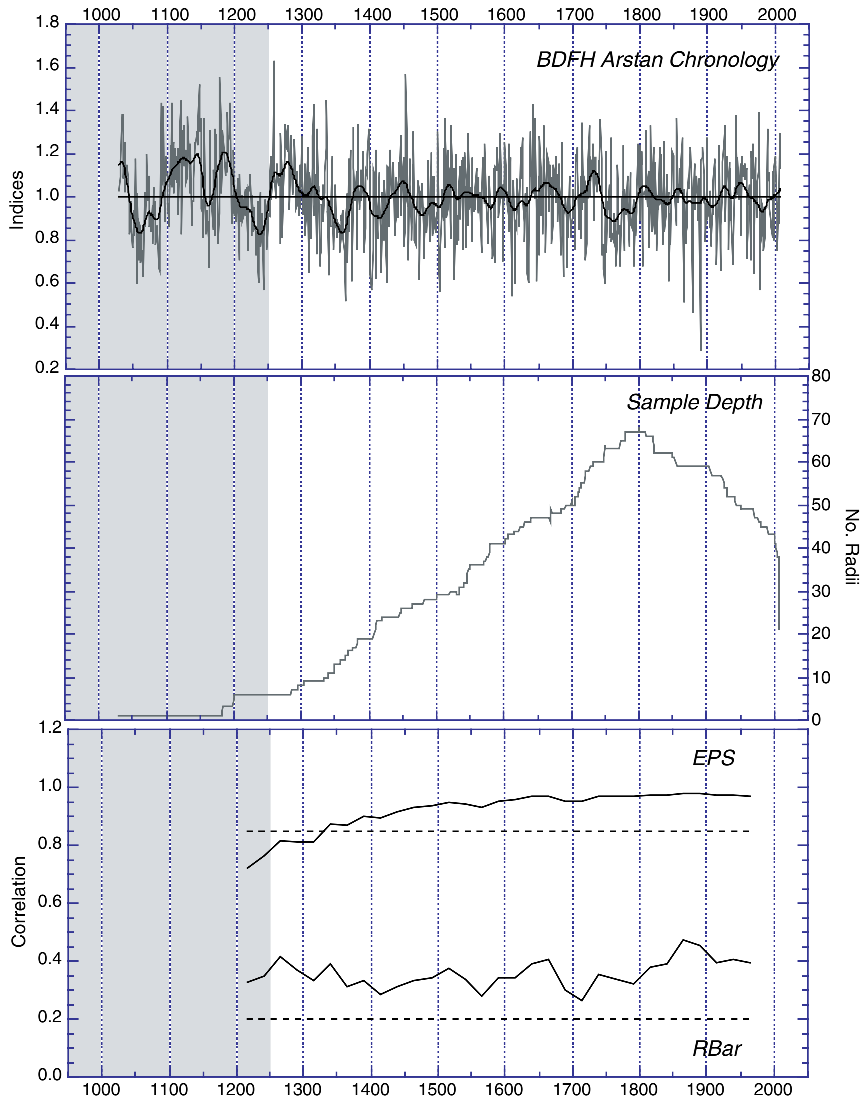

Fig. S1. The Bidoup Nui Ba Fokienia Hodginsii (BDFH) *Fokienia hodginsii* chronology indices are shown in the top plot, with sample depth (center) and two measures of signal strength through time shown in the bottom plot: the Expressed Population Signal and the mean Rbar. The dashed lines show the level of accepted confidence for each of these two statistics. The shaded gray box indicates the period from 1030 to 1250 CE when the sample depth is low and less confidence is placed in the chronology. This is the longest and most well replicated tree ring record yet produced from the tropics.

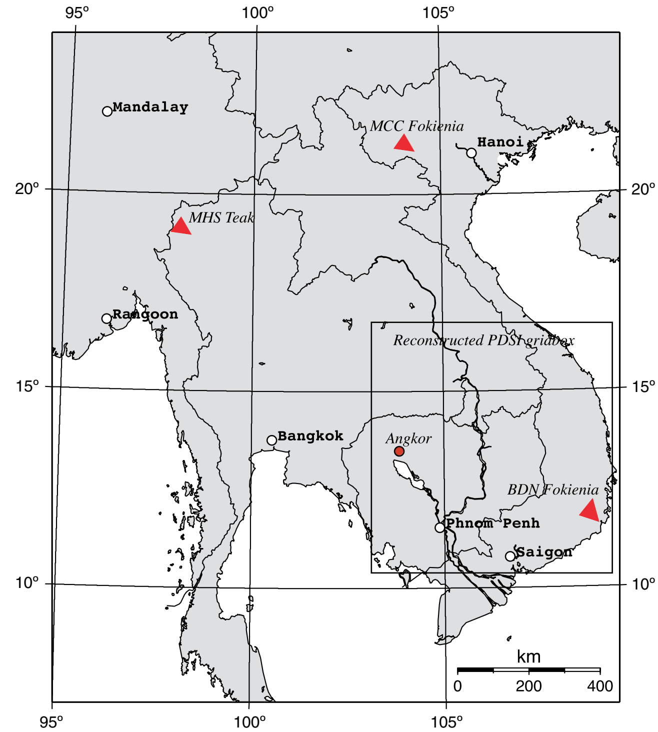

Fig. S2. The locations of the three drought records discussed in this paper are marked by the red triangles, while the nine gridpoints of the Dai Palmer Drought Severity Index (PDSI) that were averaged for use in our reconstruction are enclosed within the black square. Note the location of Angkor on the northern shore of the seasonally variable Tonle Sap, a body of water that increases its area each season with the advance of the monsoon. Stronger monsoons increase the overall size of the lake and hence its proximity to Angkor itself. During dry seasons the lake recedes by several kilometers.

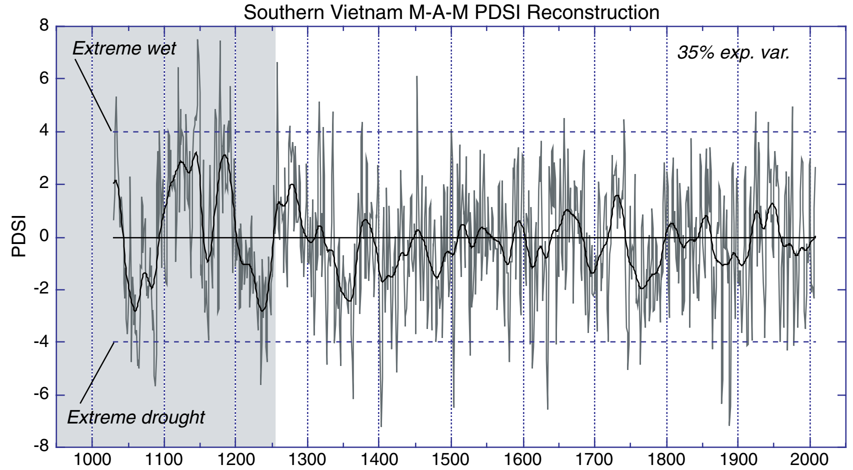

Fig. S3. The full PDSI reconstruction back to 1030 CE, explaining around 35% of the variance in the original PDSI nine-gridbox average data. The area shaded in gray, prior to 1250 CE, is considered less reliable due to decreased sample size, and the corresponding reduction in the EPS and RBAR statistics and shown in Fig. S1. However, we note that the overall trend and multidecadal structure of the reconstruction implies wetter than average conditions throughout key portions of the Medieval Warm Period, consistent with La Niña-like base state conditions.

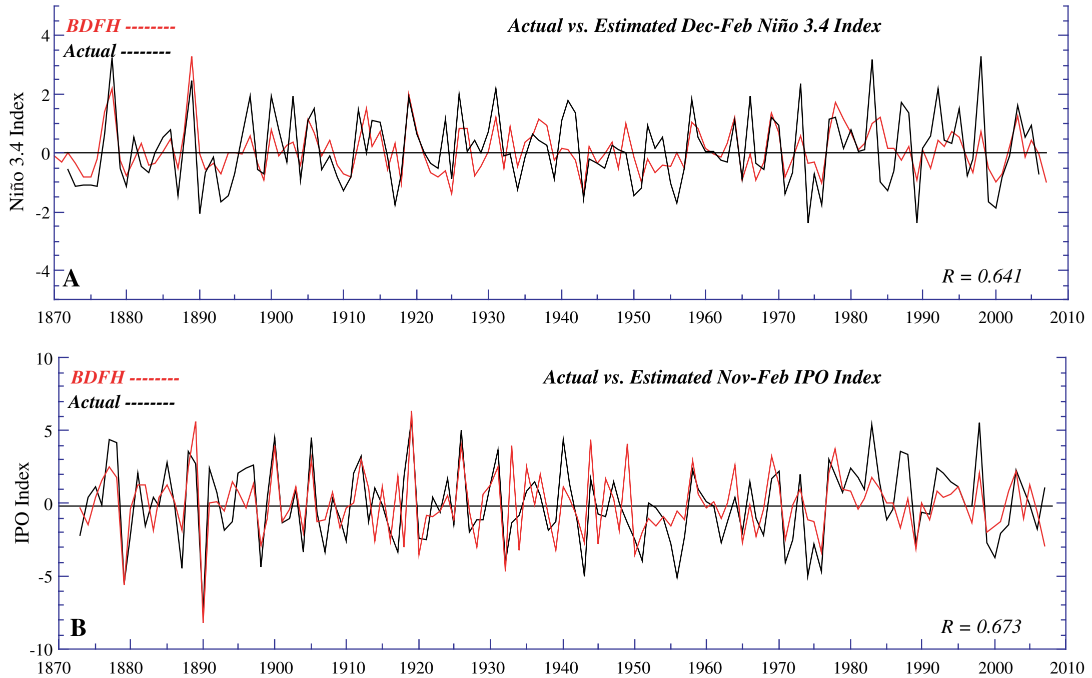

Fig. S4. Comparison plots between BDFH and (*A*) Niño 3.4 Index, and (*B*) against the Interdecadal Pacific Oscillation Index. Correlation coefficients are shown in the lower right corner of each plot. The relationship with both records shows remarkable stability throughout the entire period of record.

Table S1. Calibration and verification period statistics for the reconstructed PDSI values from the nine-gridbox average over southern Vietnam and Cambodia

Test	Score	t stat	Probability
Equality of means	0.000 (−0.048)	0.000 (−0.122)	0.99570 (0.89869)
Cross products mean	1.884 (1.840)	3.949 (3.115)	0.00017 (0.00167)
Sign test	35+ 11− (33+ 12−)	^{z}3.391(2.981)	0.00035 (0.00143)
Pearson correlation	$r = 0.581$(0.568)	4.733 (4.524)	0.00002 (0.00004)
Robust correlation	$r = 0.586$(0.550)	4.792 (4.323)	0.00002 (0.00006)
Spearman correlation	$r = 0.603$(0.589)	5.018 (4.778)	0.00001 (0.00002)
Kendall TAU	$t = 0.424$(0.400)	^{z}4.157(3.874)	0.00002 (0.00005)
Reduction of error	0.377 (0.322)		
Coefficient of efficiency	0.337 (0.322)		

Verification period 1915–1959.

Test	Score	t stat	Probability
Equality of means	0.143 (−0.005)	0.497 (−0.016)	0.62533 (0.98420)
Cross products mean	1.149 (1.334)	3.913 (4.010)	0.00020 (0.00015)
Sign test	34+ 11− (30+ 14−)	^{z}3.280(2.261)	0.00052 (0.01187)
Pearson correlation	$r = 0.602$(0.575)	4.941 (4.550)	0.00001 (0.00003)
Robust correlation	$r = 0.614$(0.574)	5.095 (4.547)	0.00001 (0.00003)
Spearman correlation	$r = 0.632$(0.574)	5.348 (4.539)	0.00000 (0.00004)
Kendall TAU	$t = 0.442$(0.397)	^{z}4.285(3.803)	0.00001 (0.00007)
Reduction of error	0.419 (0.328)		
Coefficient of efficiency	0.303 (0.327)		

The calibration period is 1960–2005, verification on 1915–1959, undifferenced (1st-differenced), ^{z} = z-score. All tests are passed, even for Reduction of Error and Coefficient of Efficiency in the verification period, the latter a notoriously difficult test to pass. The reconstruction shows remarkable stability across both time periods, in spite of data quality issues within the PDSI instrumental record itself.

Table S2. The 40 driest (*Left*) and wettest (*Right*) years of the entire 759-year reconstruction

40 Driest years				40 Wettest years			
Year	PDSI	Year	PDSI	Year	PDSI	Year	PDSI
1403	**−7.209**	1582	−4.684	1258	6.657	1274	3.577
*1888	−7.151	1633	−4.659	**1453**	**6.111**	1512	3.487
1402	**−6.878**	1526	−4.519	**1316**	**5.158**	1276	3.486
1634	−6.538	1969	−4.312	1975	4.968	1283	3.445
1503	−6.480	**1416**	**−4.287**	1257	4.794	1593	3.437
*1889	−6.464	**1417**	**−4.254**	1924	4.786	1861	3.412
*1877	−6.348	1864	−4.253	**1335**	**4.745**	1943	3.404
1363	**−6.174**	**1327**	**−4.237**	1657	4.546	1641	3.396
1635	−5.909	1615	−4.196	1741	4.463	1663	3.387
*1878	−5.413	**1401**	**−4.196**	1942	4.380	**1336**	**3.371**
1404	**−5.380**	1978	−4.138	**1376**	**4.364**	1855	3.354
1504	−5.272	1912	−4.113	1658	4.356	1923	3.346
1424	**−5.123**	1977	−4.096	1275	4.240	1540	3.329
1746	−5.023	1646	−4.096	**1322**	**4.198**	1685	3.313
1614	−4.990	1747	−4.096	1500	4.082	1640	3.279
1346	**−4.891**	1610	−4.080	**1375**	**3.817**	1951	3.263
1764	−4.858	1913	−4.072	1835	3.751	1929	3.188
1326	**−4.841**	**1338**	**−4.047**	1625	3.668	1742	3.188
1581	−4.775	1865	−4.039	1279	3.619	1546	3.172
1362	**−4.750**	1958	−3.989	1928	3.602	1847	3.155

The bold values denote those years that fall within the two Angkor drought periods in the mid-1300s and early 1400s, respectively. It is apparent that some of the driest and wettest years fall within these periods, indicating great climate instability. The asterisks mark the four years associated with two big El Niño warm episode events from the instrumental record (1877–1878 and 1888–1889), which were responsible for the Great Victorian Droughts, and these all fall among the 10 driest years of the past seven and a half centuries. The two wettest years, 1258 and 1453, coincide with the two biggest tropical volcanic eruptions of the past millennium.